Inorganic Chemistry

ARTICLE

pubs.acs.org/IC

$CsTe_2O_{6-x}$: Novel Mixed-Valence Tellurium Oxides with Framework-Deficient Pyrochlore-Related Structure

Theeranun Siritanon,[†] Jun Li,[†] Judith K. Stalick,[‡] Robin T. Macaluso,[§] Arthur W. Sleight,[†] and M. A. Subramanian[†,*]

[†]Department of Chemistry, Oregon State University, Corvallis, Oregon 97331, United States

[‡]NIST Center for Neutron Research, National Institute of Standards and Technology, 100 Bureau Drive MS 6102, Gaithersburg, Maryland 20899-6102, United States

[§]School of Chemistry and Biochemistry, University of Northern Colorado, Greeley, Colorado 80639, United States

Supporting Information

ABSTRACT: Structures of $CsTe_2O_{6-x}$ phases were investigated by single-crystal X-ray diffraction and neutron powder diffraction. Stoichiometric $CsTe_2O_6$ is a mixed-valence $Cs_2Te^{4+}Te_3^{6+}O_{12}$ compound with a rhombohedral pyrochlore-type structure where there is complete order of Te^{4+} and Te^{6+}. On heating, this compound develops significant electrical conductivity. As $CsTe_2O_6$ becomes oxygen deficient above 600 °C, the rhombohedral pyrochlore-type structure is replaced by a cubic pyrochlore-type structure with disordered Te^{4+}/Te^{6+} and oxygen vacancies. However, for $CsTe_2O_{6-x}$ phases prepared at 500 °C, the observed pyrochlore-type structure has orthorhombic symmetry. The Te^{4+} and O vacancies are all on chains running along the *b* axis, and the maximum value of *x* observed is about 0.3. At still higher values of *x* a new compound was discovered with a structure related to that reported for $Rb_4Te_3^{4+}Te_5^{6+}O_{23}$.

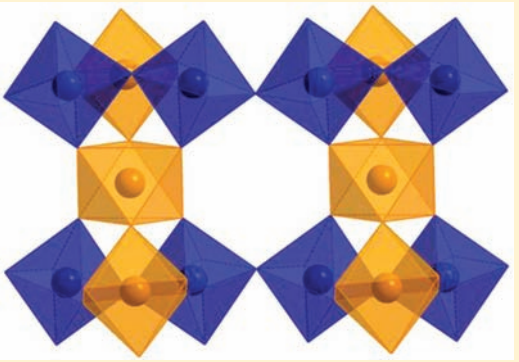

INTRODUCTION

In 1986 Loopstra and Goubitz[1] reported the structures of four Cs−Te oxides. Three of these contain only Te^{4+}: Cs_2TeO_3, $Cs_2Te_2O_5$, and $Cs_2Te_4O_9$. The fourth compound, $CsTe_2O_6$, contains mixed-valence Te and can be written as $Cs_2Te^{4+}Te_3^{6+}O_{12}$. This compound has a pyrochlore-type structure also known for various cubic CsM_2O_6 and CsM_2O_5F compounds such as $CsNbWO_6$ and $CsTa_2O_5F$.[2] However, $Cs_2Te^{4+}Te_3^{6+}O_{12}$ has an ordered arrangement of Te^{4+} and Te^{6+}, which reduces the symmetry from cubic to rhombohedral[1,3] (Figure 1). Such an ordering has never been observed for other $A_2M^{4+}M_3^{6+}O_{12}$ pyrochlores such as $Cs_2Ti^{4+}W_3^{6+}O_{12}$.[4] More remarkably, the Te^{4+} site in this rhombohedral structure is an inversion center. This is apparently the only example of a $5s^2$ cation at such high symmetry in an oxide. Ordinarily, one expects to see a low-symmetry site that provides space on one side of the cation for the lone pair electrons.

In 2001 a second modification of $CsTe_2O_6$ was reported.[5] The structure was again pyrochlore type but now in the usual cubic structure with just one site for the mixed-valence Te. For two compounds with the same $CsTe_2O_6$ formula, one form must be more thermodynamically stable at a given temperature and pressure. Given the existence of an ordered form of $CsTe_2O_6$ at room temperature, it is difficult to understand how a disordered form could also exist at room temperature. The ordered form should be of lower energy. No diffusion of cations is required for Te^{4+} and Te^{6+} to order. Only electrons would need to move for this ordering to occur, providing an easy route to the ordered structure. It should not be possible to quench in a disordered form. A primary motivation of this study was to understand the existence of this cubic form of "$CsTe_2O_6$". Another motivation was our search for another superconductor based on a mixture of s^0 and s^2 configurations, such as occurs in Ba(Bi, Pb)O_3.[6] Superconductivity is not well known in the pyrochlore structure but does occur in $CsOs_2O_6$.[7]

EXPERIMENTAL SECTION

$CsTe_2O_6$ was prepared by heating a stoichiometric mixture of $CsNO_3$ (Alfa Aesar, 99.8%) and TeO_2 (Aldrich, 99+%) in air at 600 °C for 12 h. Cs_2CO_3 (Alfa Aesar, 99.9%) and TeO_2 were used to prepare $CsTe_2O_{4.5}$ by solid state reaction at 500 °C for 12 h under Ar. To prepare polycrystalline samples of $CsTe_2O_{6-x}$ with $x = 0.25-1.15$, appropriate amounts of $CsTe_2O_6$ and $CsTe_2O_{4.5}$ were reacted in evacuated and sealed silica tubes at 500 °C for 12 h. All samples were characterized by powder X-ray diffraction (XRD) collected on a Rigaku MiniFlex II powder diffractometer using Cu Kα radiation and a graphite monochromator on the diffracted beam. Thermogravimetric analyses (TGA) were performed on a Mettler Toledo TGA 850. The diffuse reflectance spectra were obtained in the range of 200−1100 nm using a Xe lamp

Received: May 23, 2011
Published: July 27, 2011

ACS Publications © 2011 American Chemical Society

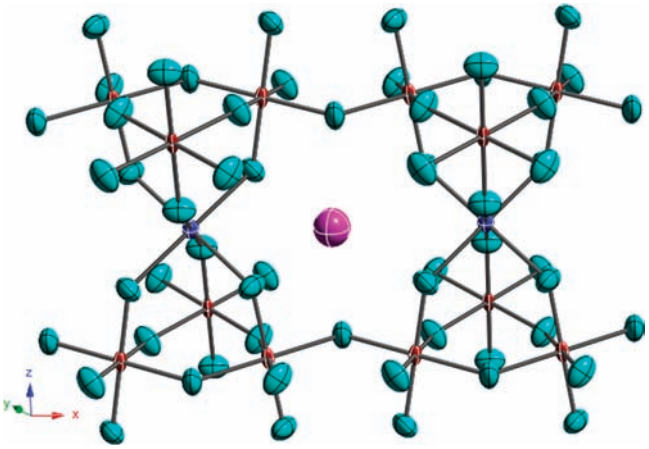

Figure 1. Crystal structure of rhombohedral $CsTe_2O_6$ showing ordering of Te^{4+} (blue) and Te^{6+} (brown) and anisotropic thermal ellipsoids of Cs (magenta), Te, and O (turquoise).

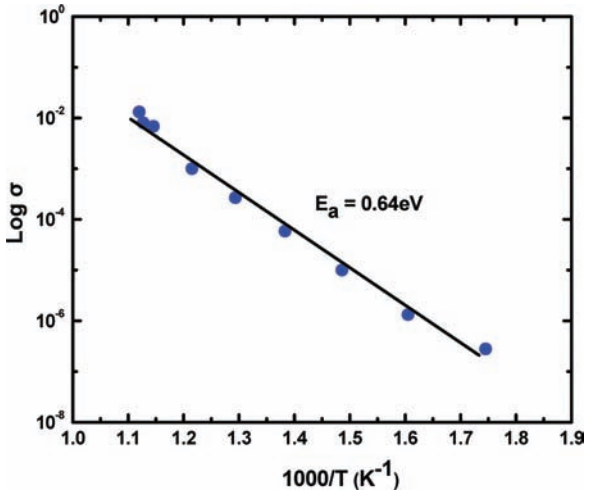

Figure 2. Electrical conductivity (log scale) vs $1000/T$ for $CsTe_2O_6$. Standard uncertainties are not indicated but are less than the point size.

with a grating double monochromator. Diffuse light reflected by the samples was collected with an integrating sphere and detected with a Si diode detector. $BaSO_4$ was used as a reference to normalize the data. The Kebulka−Munk function was used to transform reflectance data to absorbance. High-temperature resistivity was measured by the 2-probe method using platinum electrodes. The pellet was sandwiched between two sheets of Pt, which were connected to a multimeter through platinum wire. A temperature-programmable furnace was used to heat the sample.

A single crystal of cubic $CsTe_2O_{6-x}$ was obtained from a partially melted pellet of $CsTe_2O_6$ that had been heated above 600 °C. Crystals of rhombohedral $CsTe_2O_6$ were prepared by chemical vapor transport using $TeCl_4$ as a transporting agent. Reactants were weighted in an Ar-filled glovebox and loaded into a silica tube (1 cm diameter and 15 cm length) that was evacuated and sealed. The zones of the two-zone furnace were set at 620 and 590 °C. The tube was kept at these temperatures for 120 h before being cooled to 450/480 °C at 0.1 °C/min and then cooled to room temperature at 5 °C/min. Rhombohedral $CsTe_2O_6$ crystals formed in the hot end of the tube.

Single-crystal X-ray diffraction data were collected on a Bruker SMART APEXII CCD system using an Oxford Cyrostream cooler. A standard focus tube was used with an anode power of 50 kV at 30 mA, a crystal to plate distance of 5.0 cm, 512 × 512 pixels/frame, beam center (256.52, 253.16), ϕ/ω scan with step of 0.30°, exposure/frame of 10.0 s/frame, and SAINT integration. The SADABS program was used to correct for absorption. The crystal structures were solved by the direct method using the SHELXS program and refined by the full-matrix least-squares method using SHELXTL software.[8]

Neutron diffraction data were collected on three samples. A sample of $CsTe_2O_6$ was prepared in air as described above, and a sample of $CsTe_2O_{5.75}$ was prepared in a silica ampule as described above. The third sample was prepared by placing $CsTe_2O_6$ in the furnace previously heated to 610 °C, holding for 2 h, and then quenching to room temperature. This procedure was repeated for 2.5 h and again for 2 h. Neutron powder diffraction data were collected using the BT-1 32-counter high-resolution diffractometer at the NIST Center for Neutron Research at the National Institute of Standards and Technology. A Cu (311) monochromator, yielding a wavelength of 1.5401(2) Å, was employed. Collimation of 15′ of arc was used before the monochromator, 20′ before the sample, and 7′ before the detectors. The samples were loaded into vanadium containers 15.8 mm in diameter and 50 mm in length. Data were collected at room temperature over a 2θ range from 3° to 168°. Neutron diffraction data were refined by the Rietveld method using GSAS software.[9]

RESULTS

$CsTe_2O_6$. Given the highly unusual rhombohedral structure reported for $CsTe_2O_6$, further investigation of the structure of this form was deemed appropriate. We refined this structure from both single-crystal X-ray diffraction data collected at 110 K and powder neutron diffraction data collected at room temperature. In both cases the original structure reported was fully supported, and the corresponding CIF files are included in the Supporting Information. However, refinement of anisotropic displacement factors was not given in the previous report on the structure of $CsTe_2O_6$.[1] Such thermal ellipsoids could potentially give information about a tendency for Te^{4+} to exhibit the typical lone pair distortion. Despite the high symmetry of the Te^{4+} site, a thermal ellipsoid at this site is allowed to either elongate or flatten along the 3-fold axis. In fact, the ellipsoid for Te^{4+} is close to spherical, being only slightly flattened along the 3-fold axis (Figure 1). All thermal ellipsoids are unremarkable, indicating a completely normal structure. The neutron data are especially sensitive to the contribution from oxygen. Refinement of occupancies indicates that both O sites are fully occupied (Rietveld refinement plot is provided in the Supporting Information). Although the electrical conductivity of a $CsTe_2O_6$ pellet was too low to measure at room temperature, it became measurable above 300 °C (Figure 2).

$CsTe_2O_{6-x}$. The oxygen-deficient $CsTe_2O_{6-x}$ samples could be prepared by heating $CsTe_2O_6$ above 600 °C or by controlling the oxygen content in sealed silica ampules starting from stoichiometric mixtures of $CsTe_2O_6$ and $CsTe_2O_{4.5}$. We have been unable to dissolve these samples for titrations that might give an accurate value of x based on Te^{4+} content. Although the silica ampules containing the reactants were evacuated before sealing, some O_2 may evolve on heating. The values of x are somewhat dependent on the amount of O_2 gas in these ampules, which is unknown and will be somewhat temperature dependent. Some checks on the actual value of x were obtained by TGA (Figure 3) and refinement of O occupancies from diffraction data.

Figure 4 shows the powder XRD patterns of $CsTe_2O_{6-x}$ compositions prepared in silica ampules. A pseudocubic phase with a pyrochlore-type structure exists over an apparent range of about $CsTe_2O_{5.8}$ to $CsTe_2O_{5.7}$. Peak splitting and broadening is

dx.doi.org/10.1021/ic2010375 |Inorg. Chem. 2011, 50, 8494–8501

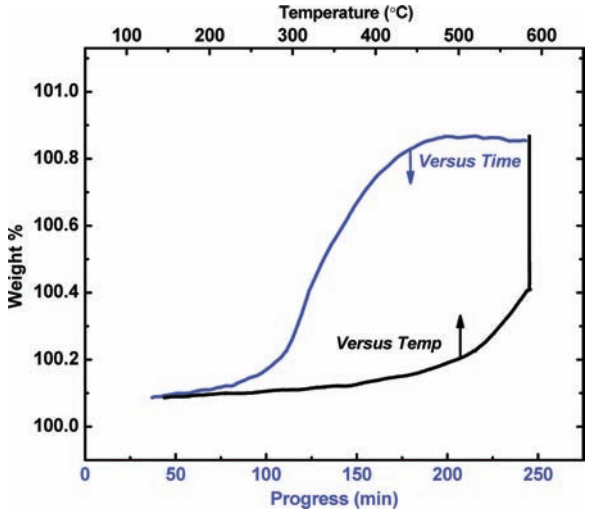

Figure 3. Thermogravimetric analysis (TGA) of nominal $CsTe_2O_{5.75}$ phase under O_2 atmosphere showing weight gain corresponding to $x = 0.25$ in $CsTe_2O_{6-x}$.

observed, indicating that the symmetry is actually not cubic. The $CsTe_2O_{5.9}$ composition is a mixture of rhombohedral $CsTe_2O_6$ and pseudocubic $CsTe_2O_{5.8}$, thus showing the miscibility gap between these two phases. Several lower symmetries were evaluated for pseudocubic $CsTe_2O_{6-x}$, and the best Rietveld fits of powder XRD and neutron patterns were obtained with an orthorhombic cell based on a space group of *Imma* or *Pnma*. Many fluorides of the type $A^{1+}M^{2+}M^{3+}F_6$ (A^{1+} = Cs, Rb, K, NH_4; M^{2+} = Mg, Zn, Fe, Ni, Co, Cu, Ag; M^{3+} = Fe, Ni, Cu, V, Co, Cr, Al, In) have been reported with an orthorhombically distorted pyrochlore-type structure.[10−13] Most have the *Pnma* space group, but some have the *Imma* space group. In both cases, the structure can be viewed as chains of M^{2+} cations running perpendicular to M^{3+} chains. This orthorhombic pyrochlore-type structure has apparently never been reported for an oxide. The *Pnma* structure is a rather minor distortion of the *Imma* structure. Thus, the peaks violating the body-centered absence condition are weak, and we cannot be absolutely certain of their presence due to weak impurity peaks in our pattern. When we refine the structure in *Pnma* the positions of Cs and Te1 remain very close to the positions they would have in *Imma*. However, some O positions deviate significantly from the positions they would be constrained to in *Imma*. Thus, we present the structure in *Pnma*. However, our Rietveld refinements in *Imma* produce the same conclusions concerning the O site with O vacancies and the strong displacement of Te toward this vacancy. Our neutron diffraction data were collected on a sample with a nominal composition of $CsTe_2O_{5.75}$. Resulting interatomic distances and site occupancies are summarized in Tables 1 and 2 (Rietveld refinement plot is provided in the Supporting Information). One Te site has a significantly larger average Te−O distance than the other site, 2.00 Å for Te2 vs 1.92 Å for Te1. The smaller average Te−O distance is typical of Te^{6+} and essentially the same average distance we find for Te^{6+} in $CsTe_2O_6$ (1.921 Å). The larger distance is indicative of some larger Te^{4+} on this site along with Te^{6+}. The O vacancies are predominantly only on the O2 site, and the O occupancy for O2 refined to be 74% is in good agreement with the nominal composition of $CsTe_2O_{5.75}$. On the basis of the hypothesis that Te atoms next to an O

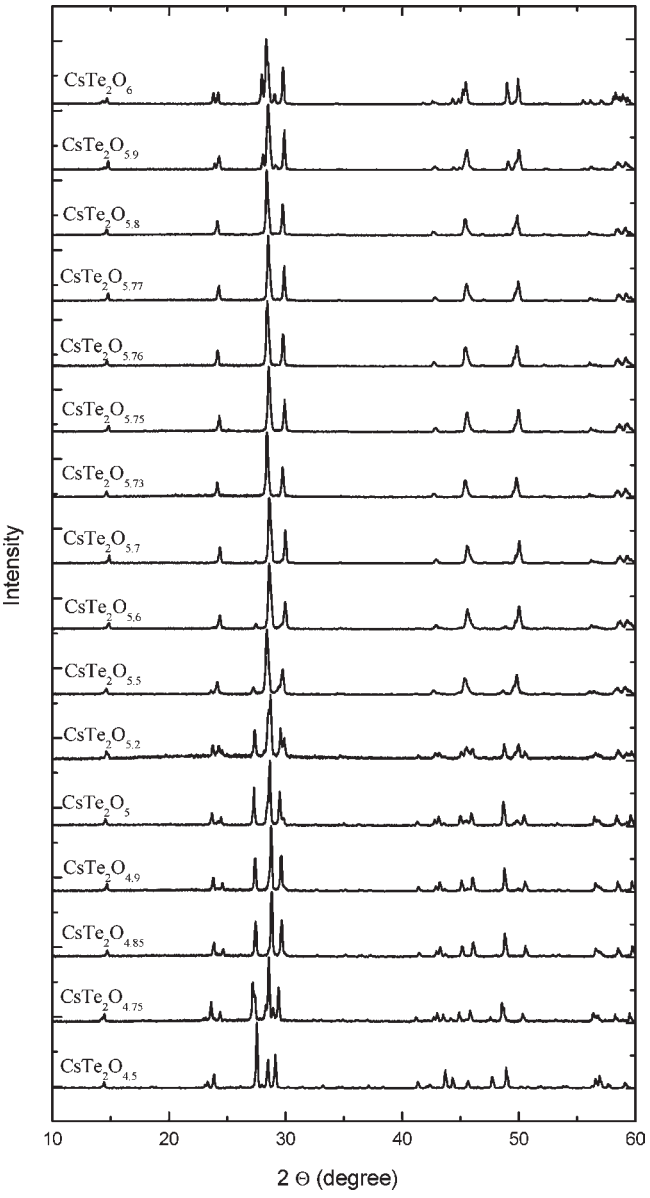

Figure 4. Powder XRD patterns of $CsTe_2O_{6-x}$ compositions prepared in silica ampules. Powder XRD pattern of pseudocubic phase showing peak splitting and broadening is provided in the Supporting Information.

vacancy would be displaced from their ideal site, this Te atom was split. The Te2 atom with no adjacent O vacancies remained fixed at its ideal position of 0,1/2,0. The added Te3 atom was allowed to move off this inversion center with *x*, *y*, and *z* all being variable. A displacement of 0.34 Å for Te3 from the inversion center occurred. Refinement of the Te2/Te3 ratio gave equal amounts of Te2 and Te3. This is the expected value for 25% vacancies on the O2 site. A section of this chain with Te^{4+} and O vacancies is shown in Figure 5. The bond valence sum[14] for Te3 is 4.47, whereas it is 4.17 for Te^{4+} in rhombohedral $CsTe_2O_6$. Refinements of anisotropic *U* values are successful for Cs, Te1, O1, O3, and O4. However, such refinement is unsuccessful for Te2, Te3, and O2. This is the part of the structure with the high degree of disorder. Our displacement of Te3 is presumed to be the largest displacement caused by this disorder, but smaller static displacements will also occur for Te2 and O2. Not surprisingly, these

dx.doi.org/10.1021/ic2010375 |*Inorg. Chem.* 2011, 50, 8494–8501

Table 1. Neutron Structural Refinement of $CsTe_2O_{5.75}$ (prepared at 500 °C)

general information						
space group						*Pnma*
a (Å)						7.3270(3)
b (Å)						7.3012(3)
c (Å)						10.2689(4)
V (Å^3)						549.34(3)
χ^2						2.87
R_p (%)						6.27
wR_p (%)						8.04
atomic coordinates and occupancies						
		x	*y*	*z*	occupancy	U_{iso} (Å^2)
Cs	Cs1	−0.0029(25)	1/4	0.6192(15)	1.0	
Te	Te1	0.246(2)	1/4	0.2472(15)	1.0	
	Te2	0	1/2	0	0.50(2)	0.011(6)
	Te3	0.013(4)	0.514(3)	0.031(3)	0.25(1)	0.005(5)
O	O1	0.4956(25)	1/4	0.192(1)	1.0	
	O2	0.014(2)	1/4	0.928(1)	0.74(2)	0.023(3)
	O3	0.2056(15)	0.4454(15)	0.130(1)	1.0	
	O4	0.803(1)	0.435(2)	0.122(2)	1.0	

thermal displacement parameters						
	U_{11} (Å^2)	U_{22} (Å^2)	U_{33} (Å^2)	U_{12} (Å^2)	U_{13} (Å^2)	U_{23} (Å^2)
Cs1	0.016(3)	0.016(3)	0.054(4)	0.0	−0.011(7)	0.0
Te1	0.001(2)	0.010(3)	0.026(5)	0.0	0.0017(25)	0.0
O1	0.005(3)	0.20(2)	0.017(5)	0.0	−0.009(6)	0.0
O3	0.050(6)	0.051(5)	0.044(5)	−0.036(4)	−0.038(4)	0.040(5)
O4	0.021(4)	0.13(1)	0.13(1)	0.027(6)	−0.007(6)	0.08(1)

Table 2. Selected Interatomic Distances (Å) for $CsTe_2O_{5.75}$

Te1−O1	1.91(2)	Cs−O1 × 2	3.727(4)
Te1−O1	1.94(2)	Cs−O1	3.20(2)
Te1−O3 × 2	1.89(1)	Cs−O2	3.17(2)
Te1−O4 × 2	1.95(2)	Cs−O2	3.57 (2)
Te2−O2 × 2	1.972(5)	Cs−O2	3.82(2)
Te2−O3 × 2	2.053(9)	Cs−O3 × 2	3.12(2)
Te2−O4 × 2	1.97(1)	Cs−O3 × 2	3.71(2)
Te3−O2	2.20(3)	Cs−O3 × 2	3.63(2)
Te3−O3	1.81(3)	Cs−O4 × 2	3.18(20)
Te3−O3	2.32(3)	Cs−O4 × 2	3.80(2)
Te3−O4	1.89(3)	Cs−O4 × 2	3.61(2)
Te3−O4	2.10(3)		

displacements are not well modeled by a thermal ellipsoid. If these displacements could be modeled, the bond valence sum for Te3 would likely be closer to 4.0. The Te2 site would be further split into two sites, one for Te^{4+} and one for Te^{6+}. The unit cell parameters and volumes for the $CsTe_2O_{6-x}$ phases prepared at 500 °C are plotted vs *x* in Figure 6. The increase in volume with increasing *x* is expected based on a $Cs_2Te_{1-x}^{4+}Te_{3-x}^{6+}O_{6-x}$ formula due to an increase of Te^{4+}, which is much larger than Te^{6+}.

Figure 7 shows the weight loss on heating $CsTe_2O_6$ in air. Separate heating and quenching experiments indicate that the products retain a pyrochlore-type structure during the initial

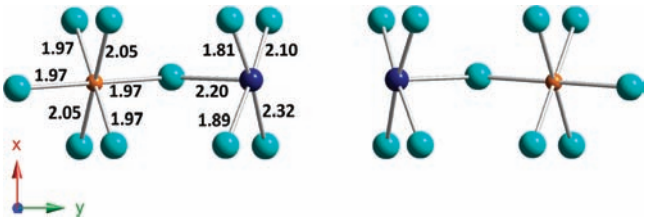

Figure 5. Segment of the chain containing the Te^{4+} and O vacancies, and the important bond distances are marked in Angstroms. The difference in the Te−O distances for the two Te atoms results from a shift of 0.34 Å for Te3 toward the O vacancy (midpoint of chain). The Te3 atoms (dark blue) are assumed to all be Te^{4+}, and the Te2 atoms (orange) are a mixture of Te^{4+} and Te^{6+}.

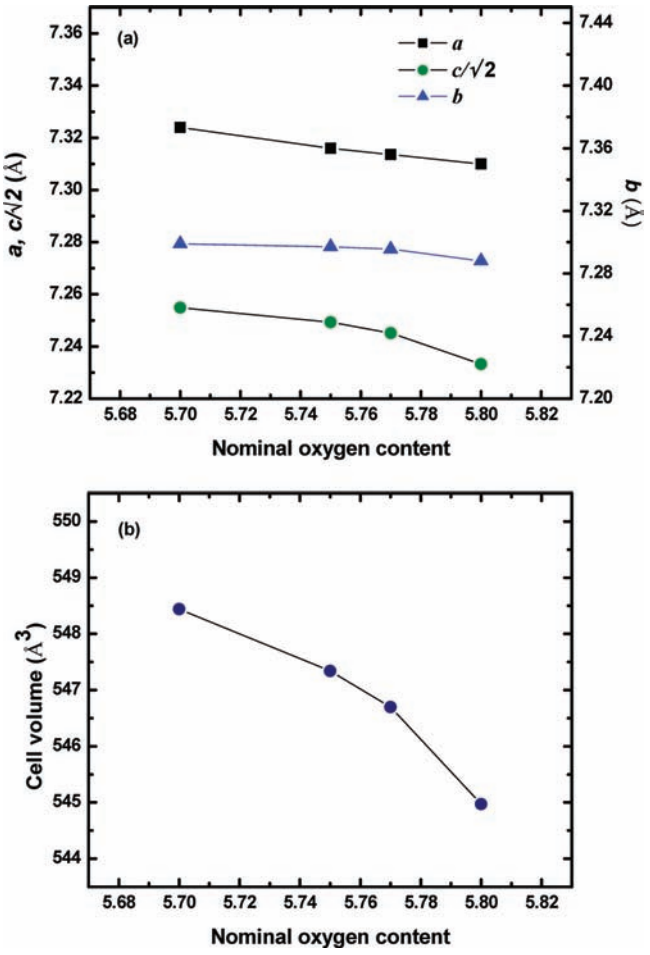

Figure 6. Lattice parameters (a) and unit cell volumes (b) of $CsTe_2O_{6-x}$ phases. Standard uncertainties are not indicated but are less than the point size.

weight loss. The discontinuity of the slope in Figure 7 at about 150 min corresponds to the disappearance of the pyrochlore-type structure for $CsTe_2O_{6-x}$ when *x* achieves about 0.25. This limit of *x* is essentially the same as that based on samples prepared in silica ampules at 500 °C. Neutron diffraction data obtained on the $CsTe_2O_{6-x}$ sample prepared by quenching from 610 °C to room temperature showed a cubic pyrochlore-type structure (Table 3). Refinement of the occupancy of the O site indicates a formula of $CsTe_2O_{5.8}$ (Rietveld refinement plot is

dx.doi.org/10.1021/ic2010375 |*Inorg. Chem.* 2011, 50, 8494–8501

provided in the Supporting Information). Structural analysis of a $CsTe_2O_{6-x}$ crystal grown at temperature > 600 °C also indicated cubic symmetry (Table 4). Refinement of the occupation of the O site for this crystal gives a formula of $CsTe_2O_{5.8}$. We conclude that the higher temperature synthesis (>600 °C) in air yields cubic pyrochlore-type phases with x values similar to that obtained in sealed ampules at 500 °C, but these phases can adopt a cubic symmetry never observed for the samples prepared at 500 °C.

$Cs_4Te_8O_{23-x}$. The isostructural mixed-valence compounds $Rb_4Te_3^{4+}Te_5^{6+}O_{23}$ and $K_4Te_3^{4+}Te_5^{6+}O_{23}$ have been reported,[15] and we have now discovered a phase of nominal composition

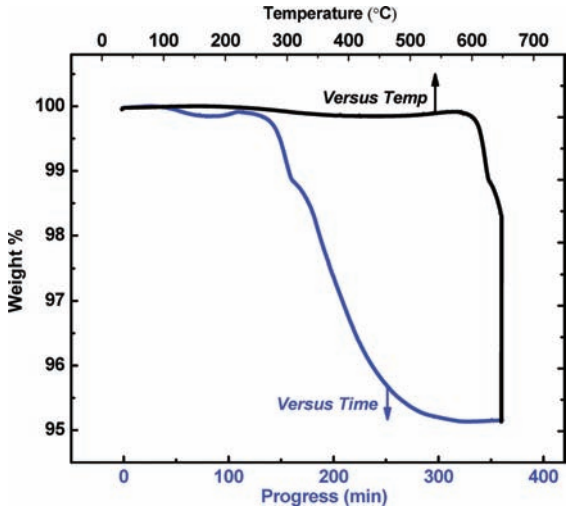

Figure 7. Thermogravimetric analysis (TGA) of $CsTe_2O_6$ in air showing weight loss.

$CsTe_2O_{4.85}$ that gives essentially the same powder X-ray diffraction pattern (Figure 8). The Cs phase apparently has significantly less oxygen than that reported for the Rb and K analogues ($ATe_2O_{5.75}$). The orthorhombic unit cell dimensions of $CsTe_2O_{4.85}$ refined by a LeBail fit of the pattern in Figure 8 are 21.783 × 14.404 × 7.190 Å. The Rb and K analogues are reported to have unit cell parameters of 19.793 × 14.664 × 7.292 Å and 19.573 × 14.448 × 7.273 Å, respectively. Only the a cell parameter of the Cs cell is larger than that reported for the Rb and K compounds. This unexpected behavior of b and c is a further indication that the stoichiometry of the Cs compound may not be the same as the Rb and K compounds. A reliable structure determination of $CsTe_2O_{4.85}$ would likely require a single crystal, as there are 105 variable positional parameters to determine.

DISCUSSION

Possible ordering schemes for different M cations in the pyrochlore structure can be visualized considering just the tetrahedral units of the M cation network. Every M cation is a member of two different tetrahedra; thus, it has 6 M near neighbors in an octahedral arrangement. On the basis of the M_4 tetrahedral unit, there are just 2 ordering schemes to consider for two different cations: A_3B and A_2B_2. Both are known to exist (Figure 9). The A_3B ordering has been observed only for $CsTe_2O_6$. The A_2B_2 ordering scheme had been known for many $A^{1+}M^{2+}M^{3+}F_6$ phases.[10−13] Now we find a variation of the A_2B_2 scheme for $CsTe_2O_{5.75}$. In the A_3B structure the B cations have no B near neighbors; all 6 near neighbors of B are A cations. The A cations have 4 A near neighbors and 2 B near neighbors. Three of the six chains defined by tetrahedral edges contain only A cations. The other three chains contain alternating A and B cations. For the A_2B_2 network there is no possible ordered

Table 3. Neutron Structural Refinement of $CsTe_2O_{5.8}$ (quenched from 610 °C)

general information					
space group					$Fd\bar{3}m$
a (Å)					10.3410(1)
V (Å^3)					1105.83(5)
χ^2/GOF					2.39
R_p (%)					6.42
wR_p (%)					8.19
atomic coordinates and occupancy					
	x	y	z		Occupancy
Cs	3/8	3/8	3/8		1.0
Te	0	0	0		1.0
O	0.3196(1)	1/8	1/8		0.97(1)
anisotropic displacement parameters					
	U_{11} (Å^2)	U_{22} (Å^2)	U_{33} (Å^2)	U_{12} (Å^2)	U_{13} (Å^2)	U_{23} (Å^2)
Cs	0.0226(7)	0.0226(7)	0.0226(7)	0.0	0.0	0.0
Te	0.0102(4)	0.0102(4)	0.0102(4)	−0.0010(4)	−0.0010(4)	−0.0010(4)
O	0.0240(8)	0.0606(8)	0.0606(8)	0.0	0.0	0.030(1)
selected bond lengths (Å) and angles (deg)						
Cs−O × 6		3.158(2)		Te−O−Te		136.99(9)
Cs−O × 12		3.7006(2)		O−Te−O		92.84(6)
Te−O × 6		1.9648(6)				

dx.doi.org/10.1021/ic2010375 |Inorg. Chem. 2011, 50, 8494–8501

Table 4. Crystallographic data of $CsTe_2O_{5.8}$ single crystal

temperature (K)	233(2)
space group	$Fd\bar{3}m$
a (Å)	10.3207(15)
V (Å^3)	1099.3(3)
abs coeff (mm^{-1})	12.823
F(000)	1242
Θ range (deg)	3.42−26.84
data/restraints/parameters	79/0/9
goodness-of-fit on F^2	1.514
final R indices [$I > 2\sigma(I)$]	R_1 = 0.0297, wR_2 = 0.0642
R indices (all data)	R_1 = 0.0297, wR_2 = 0.0642

atomic coordinates and occupancy

	x	y	z	occupancy
Cs	3/8	3/8	3/8	1.0
Te	0	0	0	1.0
O	0.320(2)	1/8	1/8	0.96(2)

anisotropic displacement parameters

	U_{11} (Å^2)	U_{22} (Å^2)	U_{33} (Å^2)	U_{12} (Å^2)	U_{13} (Å^2)	U_{23} (Å^2)
Cs	0.0249(9)	0.0249(9)	0.0249(9)	0.0	0.0	0.0
Te	0.0163(7)	0.0163(7)	0.0163(7)	−0.0029(4)	−0.0029(4)	−0.0029(4)
O	0.082(8)	0.082(8)	0.034(9)	−0.04(1)	0.0	0.0

selected bond lengths (Å) and angles (deg)

Cs−O × 6	3.15(2)	Te−O−Te	136.7(9)
Cs−O × 12	3.693(3)	O−Te−O	93.0(6)
Te−O × 6	1.963(6)		

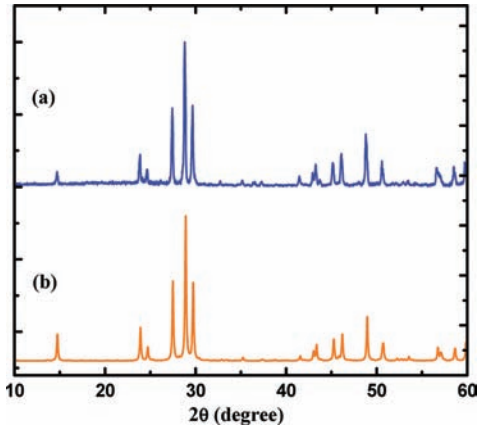

Figure 8. Observed powder XRD of nominal $CsTe_2O_{4.85}$ (a) compared with simulated pattern which was calculated based on Cs analog of $Rb_4Te_8O_{23}$ (b).

arrangement leading to either cation having all neighbors of the other type. Each of the A and B cations has 2 like and 4 unlike near neighbors. Now we have A chains running along the *a* axis and B chains running along the *b* axis. The direction of these chains is defined by the edges of the basic A_2B_2 tetrahedron. The other four edges of this A_2B_2 tetrahedron define chains with alternating A and B cations. Cubic symmetry cannot be maintained with either the A_3B- or the A_2B_2-type ordering. The symmetry drops to rhombohedral for the A_3B ordering and to orthorhombic for the A_2B_2 ordering. In the ideal pyrochlore structure the all M cations is at an inversion center. An inversion center is maintained only for the B cation in the rhombohedral structure. Inversion centers are maintained for both A and B in the *Imma* structure but only for one of these cations in the *Pnma* structure.

When $CsTe_2O_6$ becomes oxygen deficient by heating to high temperatures in air, the long-range order of Te^{4+} and Te^{6+} is disrupted and the overall lattice symmetry becomes cubic. It can be expected that Te^{4+} cations will be attracted to the disordered O vacancies. Local distortion of the lattice will occur in the vicinity of Te^{4+} and O vacancies. When $CsTe_2O_{6-x}$ phases are prepared at 500 °C, the Te^{4+} and O vacancies collect along one of the six chains. For orthorhombic $CsTe_2O_{5.75}$ there are Te1−O1 chains running along *a*, and this Te is all 6+. The Te2−O2 chains run along the *b* axis. The Te in these chains is close to 75% Te^{4+} and 25% Te^{6+}. About 25% of the O2 sites of this chain are vacant. It is O3 and O4 that bond the two chains together. The Te^{4+} is attracted to the O vacancies to provide local charge balance and a space for the lone pair of electrons. The ideal site for Te on this chain is an inversion center. However, the Te^{4+} cations on either side of this O vacancy are displaced 0.34 Å off this inversion center in the general direction of the O vacancy. This provides Te−O distances more appropriate for Te^{4+}. In this model the lone pair of electrons associated with Te^{4+} cations would become very close to one another in the region of the O vacancy. This is common behavior for lone pair cations. Close proximity of lone pairs occurs in PbO as well as in ternary oxides of Pb^{2+}.[16,17] This

dx.doi.org/10.1021/ic2010375 |*Inorg. Chem.* 2011, 50, 8494–8501

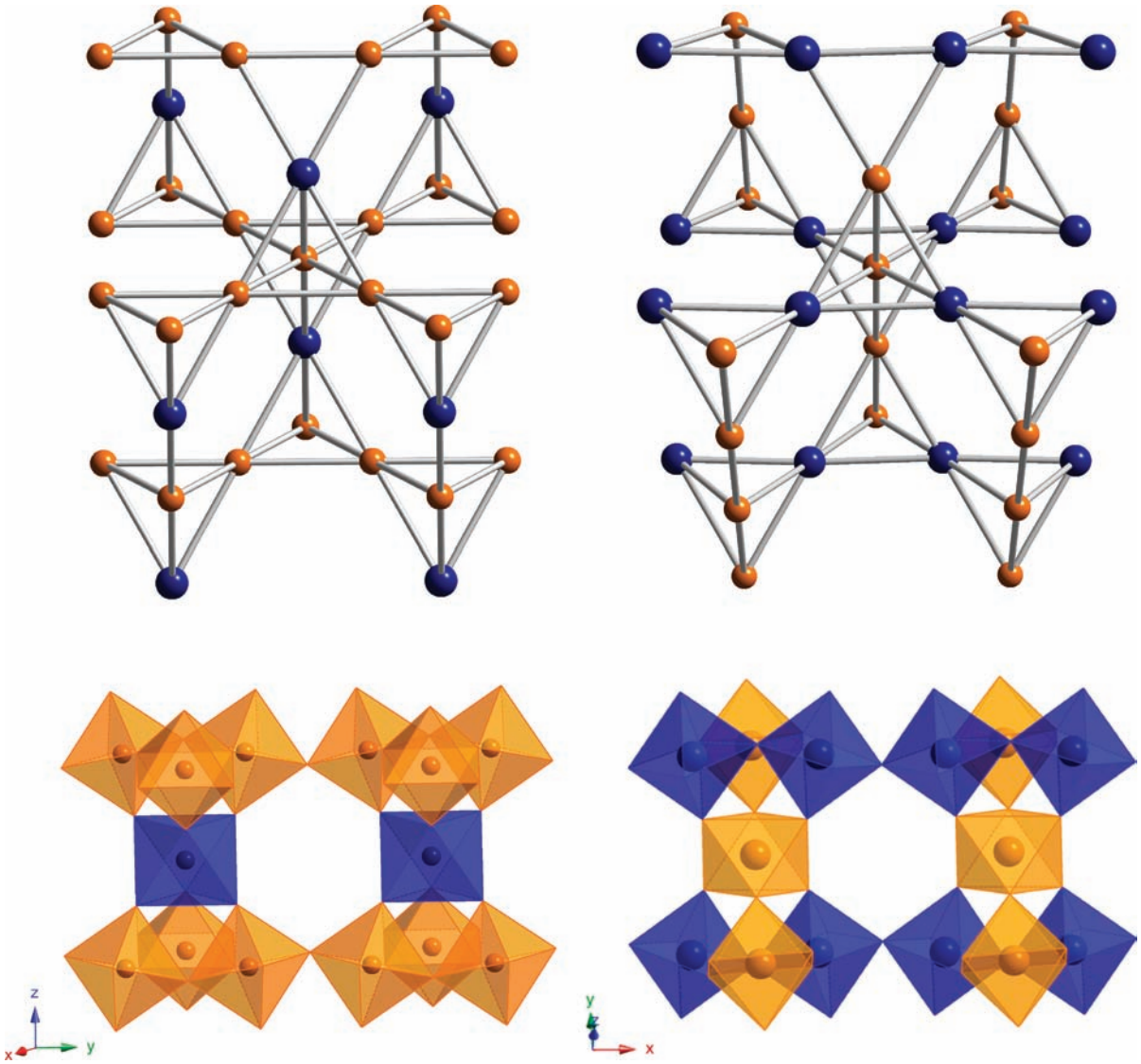

Figure 9. Arrangement of M and M′ cations in the pyrochlore structure with 1:3 (top left) and 1:1 ordering (top right). Each of the 6 edges of a tetrahedron defines a chain extended through the lattice. In the case of 1:3 ordering, 3 chains become all M cations and 3 chains become alternating M and M′ cations. In the case of 1:1 ordering, one chain is all M cations, one is all M′ cations, and the other 4 chains are alternating M and M′ cations. Bottom left and right show polyhedral arrangement of 1:3 and 1:1, respectively.

behavior is also well known in ternary oxides of Te^{4+}, with $CaTeO_3$ being a particularly good example.[18] In $CsTe_2O_{5.75}$ there are not enough O vacancies to accommodate all the Te^{4+} in positions adjacent to an O vacancy. The Te on this chain not adjacent to an O vacancy is a 1:1 mixture of Te^{4+} and Te^{6+}, and it is not so strongly displaced from the center of symmetry. However, it is likely that the environment of Te^{4+} at this site is strongly distorted relative to that of Te^{6+}. The large thermal ellipsoid of O4 (Table 1) is likely related to static displacements of O4 to provide a suitable asymmetric site for the Te^{4+} that is not adjacent to an O vacancy. If x could be increased to 0.5 for this orthorhombic pyrochlore-type structure, we would have $CsTe^{4+}Te^{6+}O_{5.5}$ where all Te^{4+} could be adjacent to an O vacancy. Oxygen vacancies are very rare in AM_2O_6 compounds with the pyrochlore structure. However, it appears that the presence of a lone pair cation, such as Te^{4+}, can stabilize O vacancies in this structure because lone pairs will effectively occupy these vacancies. In fact, $Cs_2Te_4O_9$ (or $CsTe_2O_{4.5}$) can be regarded as an example of a AM_2O_{6-x} pyrochlore with ordered O vacancies where all Te is Te^{4+}.[1]

The Te^{4+} cation in $Cs_2Te^{4+}Te_3{}^{6+}O_{12}$ is apparently the only example of a $5s^2$ cation at an inversion center in an oxide. However, the $5s^2$ cation Sb^{3+} is at an inversion center in compounds of the type $A_4Sb^{3+}Sb^{5+}X_{12}$ (A = Rb or Cs; X = Cl or Br).[19] The only example of the $6s^2$ cation Bi^{3+} at an inversion with octahedral coordination is $BaBi^{3+}Bi^{5+}O_6$.[20] These are all Type-II mixed-valence compounds according to the Robin and Day classification.[21] For Type-II mixed-valence compounds we consider $s^2 + s^0 \rightarrow 2s^1$ to be a low-energy transition due to the similarity of the environments of the s^2 and s^0 cations. All of these compounds absorb light through most or the entire visible region due to this low transition energy. It would appear that in Type-II mixed-valence compounds the mixing of the s^2 and s^0 states enhances an s^2 state that does not show the expected lone-pair distortion. Appreciable electronic conductivity for $Cs_2Te^{4+}Te_3{}^{6+}O_{12}$ develops with increasing temperature as expected for a

dx.doi.org/10.1021/ic2010375 |*Inorg. Chem.* 2011, 50, 8494–8501

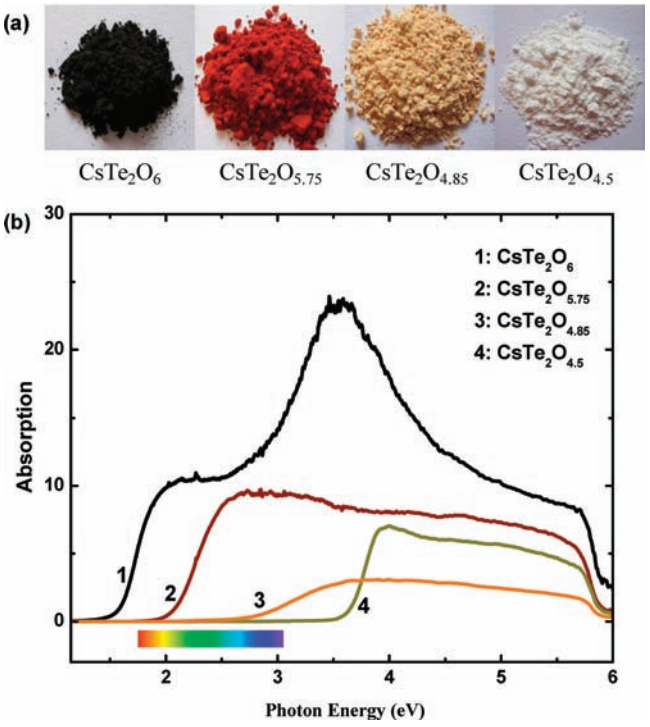

Figure 10. Colors (a) and diffuse reflectance (b) of $CsTe_2O_{6-x}$ phases.

Type-II mixed-valence compound (Figure 2). We recently reported that even higher electrical conductivity can be obtained in $Cs(Te,M)_2O_6$ pyrochlores that contain Te^{4+}.[22,23] This is caused by small M cations that compress the lattice and destabilize the s^2 state.

The color and diffuse reflectance spectra of our $CsTe_2O_{6-x}$ samples are shown in Figure 10. The red color of the orthorhombic and cubic $CsTe_2O_{6-x}$ phases and the yellow color of $Cs_4Te_8O_{23-x}$ indicate that they are Type-I mixed-valence compounds with a much higher energy $s^2 + s^0 \rightarrow 2s^1$ transition, which is due to the symmetry environment for Te^{4+} being significantly lower than that for Te^{6+}. For $CsTe_2O_{4.5}$ only Te^{4+} is present; the mixed-valence transition is gone, and the color is white.

We conclude that the "$CsTe_2O_6$" phase reported as cubic[5] was actually stabilized by a small O deficiency. Another possibility is that this cubic form was stabilized by a small substitution of a rare earth, which was present during this synthesis.

■ ASSOCIATED CONTENT

Ⓢ Supporting Information. Rietveld refinement of neutron powder diffraction of $CsTe_2O_{5.75}$, $CsTe_2O_{5.8}$, and $CsTe_2O_6$; LeBail fit of the X-ray powder diffraction pattern of $CsTe_2O_{5.75}$; crystallographic information files (CIF) of $CsTe_2O_6$ from single-crystal analysis and neutron powder diffraction refinement, $CsTe_2O_{5.8}$ and $CsTe_2O_{5.75}$ from neutron powder diffraction refinement, and $CsTe_2O_{5.8}$ from single-crystal analysis. This material is available free of charge via the Internet at http://pubs.acs.org.

■ AUTHOR INFORMATION

Corresponding Author
*E-mail: mas.subramanian@oregonstate.edu.

■ ACKNOWLEDGMENT

This work was supported by NSF grant DMR 0804167. We thank Dr. Lev Zakharov for help with single-crystal work and Dr. Janet Tate for optical data. Identification of any commercial product or trade name does not imply endorsement or recommendation by the National Institute of Standards and Technology.

■ REFERENCES

(1) Loopstra, B. O.; Goubitz, K. *Acta Crystallogr.* **1986**, *C42*, 520.
(2) Subramnaian, M. A.; Aravamudan, G.; Subba Rao, G. V. *Prog. Solid State Chem.* **1983**, *15*, 551983.
(3) Hamani, D.; Mirgorodsky, A.; Masson, O.; Merle-Méjean, T.; Colas, M.; Smirnov, M.; Thomas, P. *J. Solid State Chem.* **2011**, *184*, 637.
(4) Whittle, K. R.; Lumpkin, G. R.; Ashbrook, S. E. *J. Solid State Chem.* **2006**, *179*, 512.
(5) Weber, F. A.; Meier, S. F.; Schleid, T. *Z. Kristallogr. Suppl.* **2001**, *180*, 149.
(6) Sleight, A. W.; Gilson, J. L.; Bierstedt, P. E. *Solid State Commun.* **1975**, *17*, 27.
(7) Yonezawa, S.; Muraoka, Y.; Hiroi, Z. *J. Phys. Soc. Jpn.* **2004**, *73*, 1655.
(8) Sheldrick, G. M. *SHELEXTL*, Version 6.14; Bruker Analytical X-ray Instruments, Inc.: Madison, WI, 2003.
(9) Larson, A. C.; Von Dreele, R. B. *General Structure Analysis System (GSAS)*; Los Alamos National Laboratory Report LAUR; Los Alamos National Laboratory: Los Alamos, NM, 2004; Vol. 86, p 784. Toby, B. H. *J. Appl. Crystallogr.* **2001**, *34*, 210.
(10) Subramanian, M. A.; Marshall, W. J.; Harlow, R. L. *Mater. Res. Bull.* **1996**, *31*, 585.
(11) Friese, K.; Gesland, J. Y.; Grzechnik, A. *Z. Kristallogr.* **2005**, *220*, 614.
(12) Tressaud, A.; De Pape, R.; Portier, J.; Hagenmuller, P. *Bull. Soc. Chim. Fr.* **1970**, *10*, 3411.
(13) Ferey, G.; Leblanc, M.; de Pape, R. *J. Solid State Chem.* **1981**, *40*, 1.
(14) Lufaso, M. W.; Woodward, P. M. *Acta Crystallogr.* **2001**, *B57*, 725.
(15) Minimol, M. P.; Vidyasagar, K. *Inorg. Chem.* **2005**, *44*, 9369.
(16) Mizoguchi, H.; Ramirez, A. P.; Siegrist, T.; Zakharov, L. N.; Sleight, A. W.; Subramanian, M. A. *Chem. Mater.* **2009**, *21*, 2300.
(17) Darriet, B.; Devalette, M.; Latourrette, B. *Acta Crystallogr.* **1978**, *B34*, 3528.
(18) Stöger, B.; Matthias, W.; Zobetz, E.; Giester, G. *Acta Crystallogr.* **2009**, *B65*, 167.
(19) Prassides, K.; Day, P.; Cheetham, A. K. *Inorg. Chem.* **1985**, *24*, 545.
(20) Cox, D. E.; Sleight, A. W. *Solid State Commun.* **1976**, *19*, 969.
(21) Robin, M. B.; Day, P. *Adv. Inorg. Chem. Radiochem.* **1967**, *10*, 247.
(22) Siritanon, T.; Laurita, G.; Macaluso, R. T.; Millican, J. N.; Sleight, A. W.; Subramanian, M. A. *Chem. Mater.* **2009**, *21*, 5572.
(23) Li, J.; Siritanon, T.; Stalick, J. K.; Sleight, A. W.; Subramanian, M. A. *Inorg. Chem.* **2011**, *50*, 5747.